Supporting Information

Single-excitation dual-color coherent lasing by tuning resonance energy transfer process in porous structured nanowires

Zhaona Wang[1, *], Xiaoyu Shi[1], Ruomeng Yu[2], Sujun Wei[1], Qing Chang[1], Yanrong Wang[1], Dahe Liu[1,*]and Zhong Lin Wang[2,3]

[1]Applied Optics Beijing Area Major Laboratory, Department of Physics , Beijing Normal University, Beijing, China, 100875

[2]School of Materials Science and Engineering, Georgia Institute of Technology, Atlanta, Georgia 30332-0245, USA

[3]Beijing Institute of Nanoenergy and Nanosystems, Chinese Academy of Sciences, Beijing, China, 100083

[*]Email: zhnwang@bnu.edu.cn and dhliu@bnu.edu.cn

Contents

A: Synthesizing and characterizations of scatterer

The Ag nanowires (NWs) in our experiment are synthesized by a polyvinylpyrrolidone (PVP)-assisted reaction in ethylene glycol (EG). [1,2] 4.6 mg NaCl and 1.76 g PVP (Mw 130 000) are dissolved in 60 mL EG at 50°C, 0.68 mg $AgNO_3$ is dissolved in 40 mL EG, these two solutions are then mixed into milky form as AgCl crystal nucleus. 80 mL of this mixture is heated at 160°C for 6 h in a hot water kettle of 100 ml and then cooled down to room temperature. The derived solid material is centrifuged and washed for at least three times to remove EG and any excess PVP. The purified Ag NWs suspended in ethanol with a concentration of 7.56×10^7/ml is characterized by SEM as shown in Figure S1a, indicating a good uniformity and high aspect ratios with an averaged diameter of 80 nm and averaged length of 10μm. The inset of Figure S1a shows the absorption spectrum of Ag NWs with the peak of the surface plasmon resonance at 380 nm. We introduce a galvanic replacement reaction between Ag and $HAuCl_4$ to synthesize the Ag-Au porous NWs. A chloroauric acid ($HAuCl_4$) solution with a concentration of 4.8 mM is added into the suspension of Ag NWs with a molar ratio of $\gamma_M = M_{Au}:M_{Ag} = 0.126$. Figure S1b shows the scanning electron microscopy (SEM) image of the products for the galvanic replacement reaction, indicating that the Ag NWs are etched to form nano-gaps and plenty of Au nanoparticles are attached to form protuberances at the surfaces with high roughness.

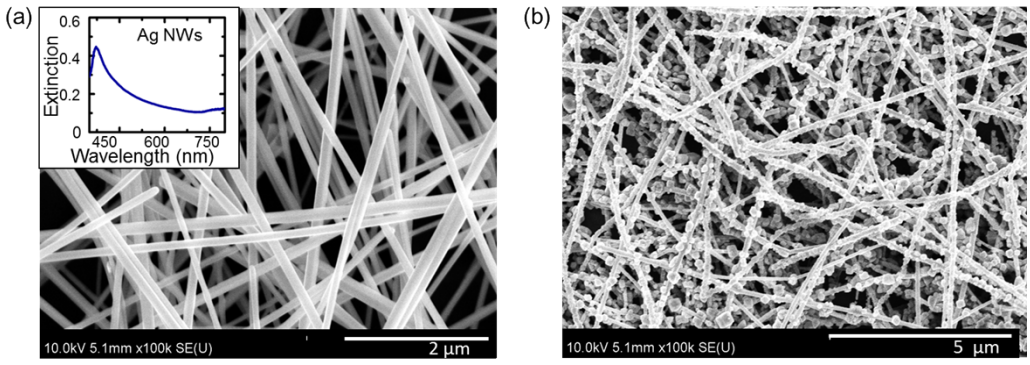

Figure S1. SEM images and extinction spectra. (a) SEM image of Ag NWs; inset is the corresponding extinction spectra (blue curve) (b) SEM image of Au-Ag NWs under the condition of $\gamma_M = M_{Au}:M_{Ag} = 0.126$.

B: Enhancement of local electromagnetic field

To illustrate the enhancement effect of local electromagnetic field by the nano-gaps formed by Au nanoparticles on the rough surface of Au-Ag NWs, we employ a two-dimentional (2D) physical model to simulate the electromagnetic field enhancement factor as ($|E|/E_0$) by using the Comsol package. In simulations, the physical model is built by setting three Au particles with diameter of 20 nm on top of an etched Ag nanowire with the diameter of 80 nm in coincidence with our real samples measured by SEM. The permittivity of Au and Ag are chosen from Johnson and Christy's experimental data.[3] The refractive index of calculation space is 1.4 for ethanol. The excitation beam is a plane wave polarized in the *x*-axis with a wavelength of 574 nm (Fig. S2c) and 638 nm (Fig. S2d). A perfectly matched layer (PML) has been chosen as boundary condition. The field enhancement factors can reach 100 at 574 nm (Fig. S2c) and 200 at 638 nm (Fig. S2d) near the nano-gaps between the Au and Ag or Au and Au. These values are much larger than that derived from a single Ag nanowires (2.4 at 574 nm and 2.3 at 638 nm as shown in Fig. S2a). The great enhancement of local electromagnetic field is formed at the nano-gaps to provide strong feedback or gain channels for the low threshold stimulated emissions from R6G and oxazine dye molecules. These results indicate that the nanostructures with abundant nano-gaps are suitable for multi-color coherent random lasing.

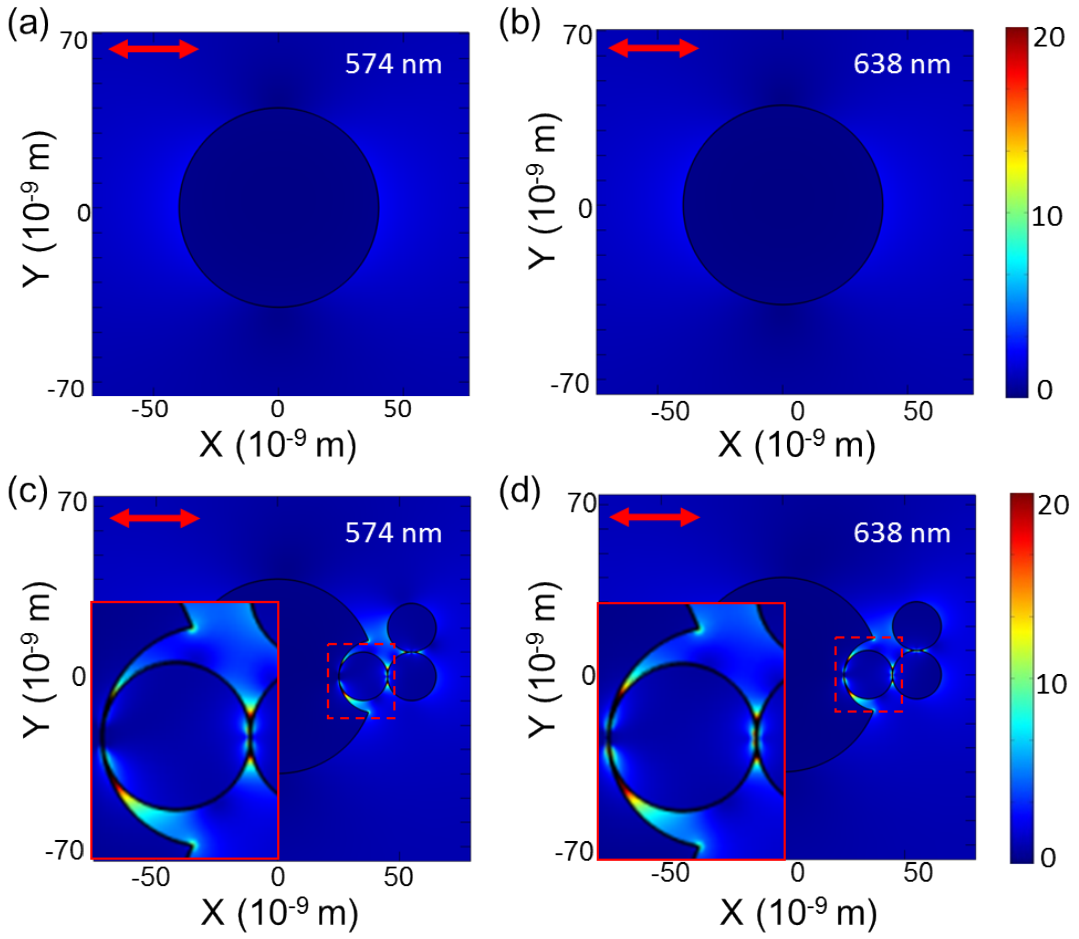

Figure S2. Enhancement of the local electromagnetic field. Electric field intensity is normalized by the incoming field near pure Ag NW for the *x*-polarized light at the wavelength of 574 nm (a) and 638 nm (b) , near Au-Ag bimetallic NWs for the *x*-polarized light at the wavelength of 574 nm (c) and at 638 nm (d).

C: Linewidths of random lasing

To demonstrate the linewidths of dual-color random lasing, the full width at half maximum (FWHM) of the lasing lines at 574.14 nm and 636.10 nm in olive in Figs. 2c and 2d is measured and shown in Fig. S3a and S3b (Supporting Information), respectively. Figure S3a shows that the FWHM of lasing lines at 574.14 nm is about 0.05 nm. The corresponding quality (Q) factor, defined as λpeak /FWHM, is about ~11,000. Figure S3b shows that the FWHM of lasing lines at 636.10 nm is about 0.06 nm. The corresponding Q factor is about ~10,000. It should be noted that these Q factors are comparable to other lasing systems with additional feedback.[4, 5]

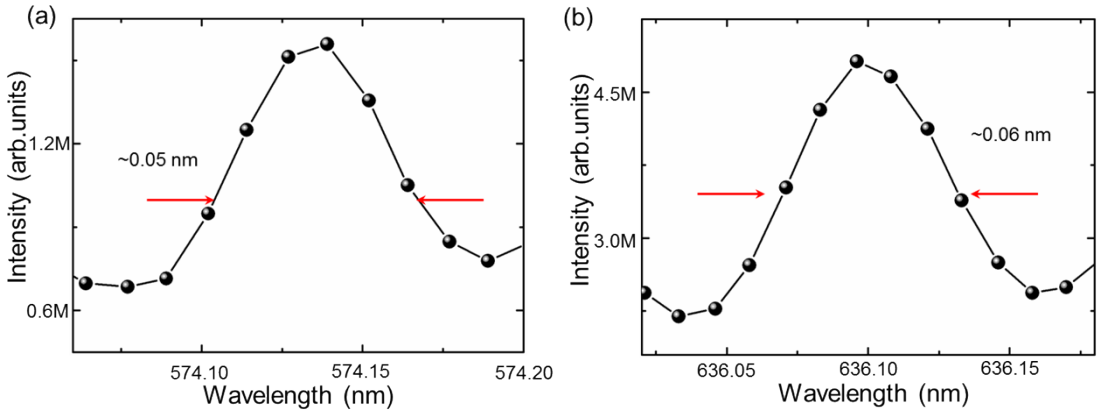

Figure S3. Linewidths of simultaneous dual-color coherent random lasing. (a) The linewidths of random lasing mode at 574.14 nm (a) and 636. 10 nm (b) from the binary-dye RET random system with R6G in the concentration of 0.43 mg/ml, oxazine in the concentration of 0.008 mg/ml and Au-Ag NWs in the concentration of 7.56×10^7/ml, pumped by 532 nm nanosecond pulsed lasers with the power density of 1.67 MW/cm^2.

D: Emission characteristic of Au-Ag NWs based single-dye R6G random system

Figure S4a presents the emission spectra of Au-Ag NWs based single-dye R6G (C_{R6G} = 0.43 mg/ml) systems under different pump power densities ranging from 0.4 to 1.02 MW/cm^2. Under weak power densities, broad influence spectra are derived indicating no lasing emitted. Under high pumping power density, sharp spikes with full width at half maximum of less than 0.1 nm are observed, indicating the emergence of coherent lasing resonance, [6,7,8] as shown by the spectrum in Figure S4a, along with the corresponding photograph as inset. The linewidth and intensity evolution of single-dye R6G system with the pump power density is shown in Figure S4b, which illustrates the emission linewidth decreases significantly to the sub-nanometer scale, while the emission intensity increases rapidly when the pump power density surpass the threshold of 0.51 MW/cm^2.

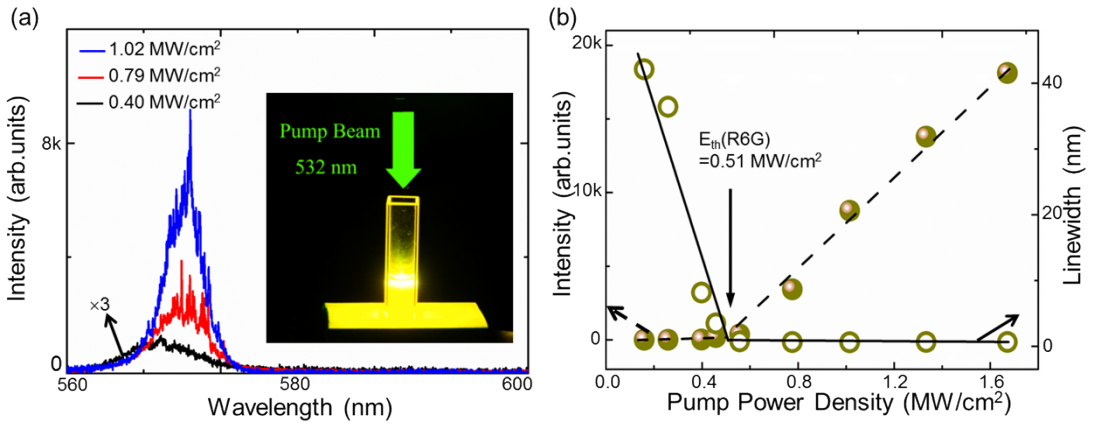

Figure S4. Emission spectra and thresholds behavior of Au-Ag NWs-based single-dye R6G systems. (a)Emission spectra and photograph of Au-Ag NWs-based single-dye R6G (C_{R6G} = 0.43 mg/ml) systems under different pump power densities. (b) The linewidth and intensity thresholds behavior of Au-Ag NWs-based single-dye R6G (C_{R6G} = 0.43 mg/ml) systems.

E: Emission characteristic of Au-Ag NWs based single-dye oxazine random system

Considering that the Au-Ag NWs-based single-dye R6G random system have strong emission at about 574 nm, which overlaps with the absorption band of oxazine, we apply a 574 nm pulse laser to directly pump the Au-Ag NWs based single-dye oxazine random systems under the same concentrate conditions to R6G@oxazine system in Fig. 2a . The emissions spectrum is presented in Fig. S5a, showing only a broad spontaneous peak, no random lasing. There is only spontaneous radiation even when the pump energy is increased to 2.53 MW/cm^2, which means 574 nm pulses cannot supply enough energy for oxazine in 0.008 mg/ml to build stimulated emissions, furtherly indicates that the energy obtained by oxazine for coherent lasing in R6G@oxazine system is majorly by the resonance energy transfer mechanism between the two dyes. Figure S5b shows the emission spectra of single-dye systems with different oxazine concentrations under the same pump pulse at 574 nm with power density of 1.33 MW/cm^2. Coherent random lasing is derived when the concentration is up to 0.1 mg/ml, which is 12.5 times larger in magnitude than that (0.008 mg/ml) in binary-dye systems.

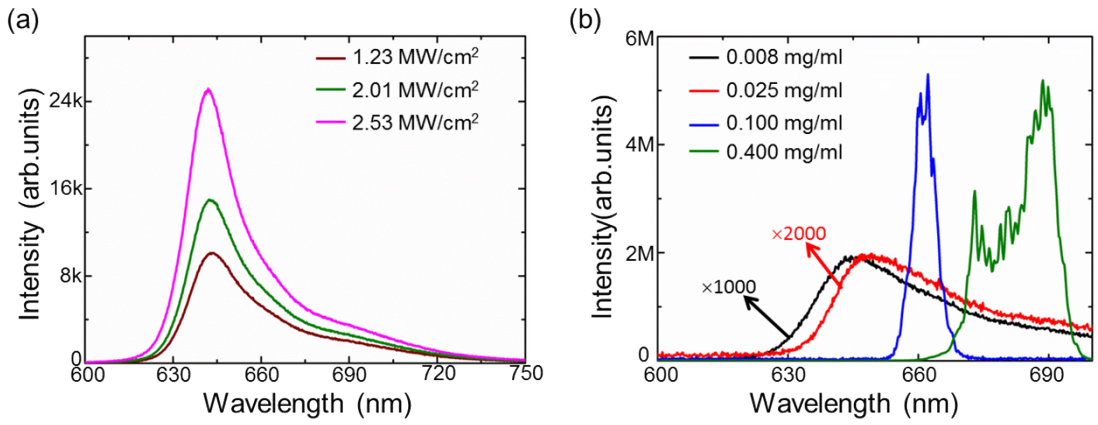

Figure S5. Emission spectra of Au-Ag NWs based single-dye oxazine systems pumped by 574 nm pulses. (a) Emission spectra of Au-Ag NWs based single-dye oxazine ($C_{Oxazine}$ =0.008 mg/ml) systems pumped by 574 nm laser beam under different pump power densities. (b) Emission spectra of Au-Ag NWs based single-dye systems with various oxazine concentrations pumped by 574 nm laser beam at the pump power density of 1.33 MW/cm^2. The spectra are obtained from the optical fiber spectrometer with a spectral resolution of 0.4 nm.

F: Transitions among three output modes under different scatterer density

To further illustrate the influence of scatterer concentrations on the relationship between output modes and mixing ratio of two dyes we reduced the concentration of Au-Ag NWs to 3.78×10^7/ml, which is half in magnitude of that employed in the main text. Transitions among three emission modes are also observed when tuning the mixing ratio between R6G and oxazine dyes. Figure S6a shows the transition process among three output modes by keeping the oxazine concentration at 0.004 mg/ml while varying the concentration of R6G from 0.1 mg/ml to 0.4 mg/ml. At a smaller C_{R6G} of 0.1 mg/ml, single chartreuse lasing output is observed; at a larger C_{R6G} of 0.2 mg/ml, the emission spectrum presents simultaneous chartreuse & red lasing output; further increasing the C_{R6G} to 0.4 mg/ml, only single red lasing is emitted. The similar results are presented in Figure S6b when fixing C_{R6G} at 0.2 mg/ml with the concentration of oxazine varying from 0.002 mg/ml to 0.01mg/ml, resulting in single chartreuse, simultaneous chartreuse & red and single red lasing output, respectively. These results indicated that the concentrations of dyes should be carefully tuned for different purposes under different concentrates of Au-Ag NWs.

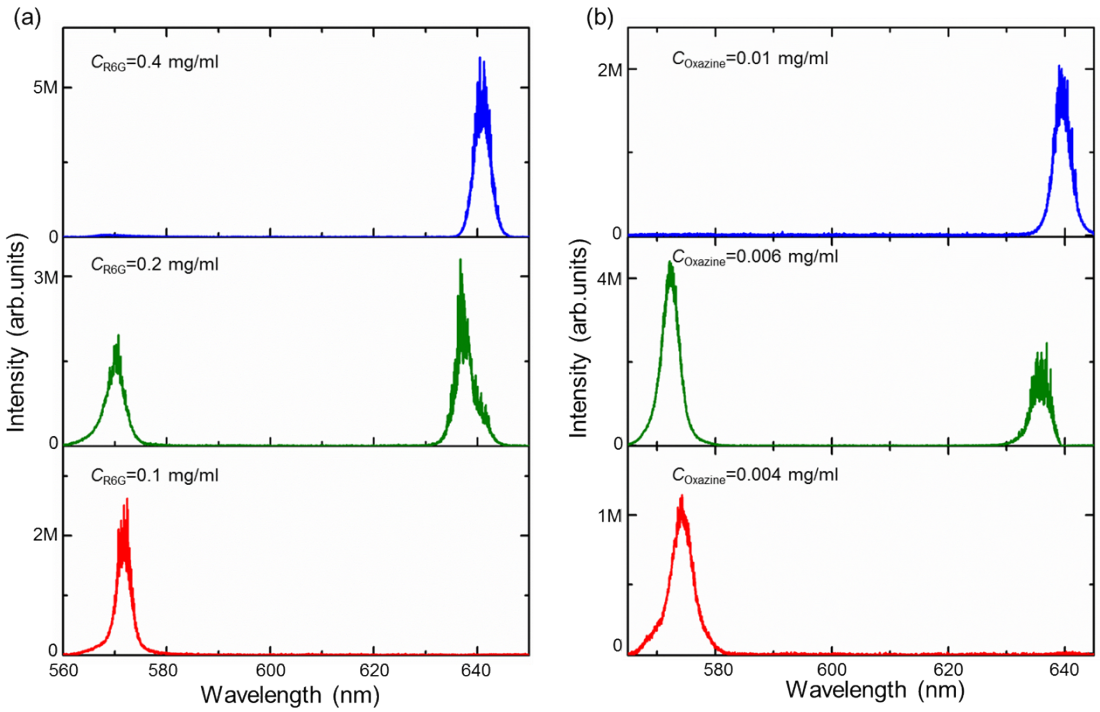

Figure S6. Transitions among three emission modes of RET based systems by tuning the mixing ratio of R6G&oxazine under Au-Ag NWs concentration of 3.78×10^7/ml. Emission spectra of RET based systems with R6G & oxazine pumped by 532 nm pulses at the power density of 1.33 MW/cm^2, (a) varying the concentration of R6G with the concentration of oxazine fixed at 0.004 mg/ml, (b) varying the concentration of oxazine with the concentration of R6G fixed at 0.2 mg/ml.

References

1. L. Gou, M. Chipara and J. M. Zaleski, *Chemistry of Materials*, 2007, **19**, 1755-1760.
2. Y. Sun, B. Gates, B. Mayers and Y. Xia, *Nano letters*, 2002, **2**, 165-168.
3. P. B. Johnson and R. W. Christy, *Phys Rev B*, 1972, **6**, 4370-4379.
4. S. Shinohara, T. Fukushima and T. Harayama, *Physical Review A*, 2008, **77**, 033807.
5. M. H. Kok, W. Lu, J. C. W. Lee, W. Y. Tam, G. K. Wong and C.-T. Chan, *Applied Physics Letters*, 2008, **92**, 151108-151108-151103.
6. H. Cao, *Journal of Physics A: Mathematical and General*, 2005, **38**, 10497-10535.
7. X. Meng, K. Fujita, Y. Zong, S. Murai and K. Tanaka, *Applied Physics Letters*, 2008, **92**, 201112.
8. X. Meng, K. Fujita, S. Murai, T. Matoba and K. Tanaka, *Nano letters*, 2011, **11**, 1374-1378.